Sensors & Transducers, Vol. 235, Issue 7, July 2019, pp. 31-36

www.sensorsportal.com

Sensors & Transducers

Published by IFSA Publishing, S. L., 2019
http://www.sensorsportal.com

Temperature Investigation of Phonon-plasmon Modes in 4H-SiC Homoepitaxial Layers

[1, 2,] Artur Dobrowolski, [1, 2,] Jakub Jagiełło, [1] Wawrzyniec Kaszub, [1] Tymoteusz Ciuk, [1] Kinga Kościewicz, [1] Paweł P. Michałowski, [1] Paweł Ciepielewski, [2] Andrzej Wysmołek, [1] Adrianna Chamryga and [1] Pawel Kamiński

[1] Łukasiewicz Research Network - Institute of Electronic Materials Technology, Wolczynska 133, Warsaw, 01-919, Poland
[2] Faculty of Physics, University of Warsaw, Pasteura 5, Warsaw, 02-093, Poland
E-mail: artur.dobrowolski@itme.edu.pl, jakub.jagiello@itme.edu.pl

Received: 15 April 2019 /Accepted: 28 May 2019 /Published: 31 July 2019

Abstract: Semiconductor devices based on silicon carbide play an important role as components for power electronic systems. Nowadays it's recognized that at least 50 percent of electricity distribution all over the world is controlled by such elements. It's also expected that within a decade, the power devices' share in electricity conversion will rise from today's 30 to 80 %. This will require next generation of energy-efficient devices for power electronics.

Keywords: SiC, Power devices, Raman spectroscopy, SIMS.

1. Introduction

In this work, we present a thorough analysis of bulk charge carrier concentration as a function of temperature, low temperature spectrum with electron transition modes in unintentionally-doped and low-doped n-type (N_2) homoepitaxial SiC layers (epi-layers) – a promising candidate for Shottky diodes. We also present a method for measuring the epi-layer thickness with Raman spectroscopy.

The epi-layers were grown at temperatures exceeding 1600˚ and rates of 5-10 μm/h on up to 3-in 4H-SiC(0001) wafers in a R&D Aixtron VP508 reactor [1, 2].

2. Measurements

We present conclusions based on results obtained with Raman spectroscopy performed using a Renishaw inVia spectrometer powered by a 532 nm Nd:YAG laser. Our results are also supported with SIMS (Secondary Ion Mass Spectrometry) that was employed to estimate the bulk concentration of nitrogen and SEM (Scanning Electron Microscopy) images [3, 4] for the epi-layer thickness comparison.

2.1. Temperature Dependence of Free arrier Concentration by Raman Spectroscopy

In this measurements we focused on temperature-induced energy line shifts of the longitudinal optical plasma-coupled (LOPC) A1. The 11-um-thick epi-layers were investigated with Raman spectroscopy from 4.6 to 300 K in vacuum conditions (Fig. 1). In a Raman spectrum of the epi-layer we can see two peaks close to 1000 cm^{-1}. The first one is related to the lower-doped epi-layer. This is the LO phonon mode. The

second one is related to the substrate and it is the LOPC which has its origin in the coupling of an optical phonon with a plasmon.

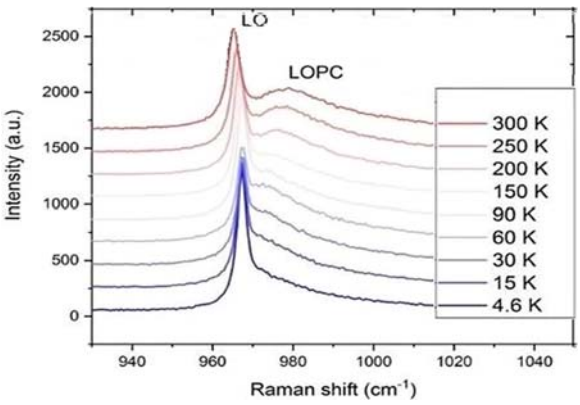

Fig. 1. Temperature dependence of the Raman spectra of the phonon (LO) and the coupled phonon-plasmon (LOPC) modes. A temperature-dependent line shift of the modes is visible.

As a result, two independent effects were observed as a function of temperature. The first was identified as thermal expansion of the crystal – which implies change of the force constant and a consequent phonon energy shift in the recorded spectra. The second one was identified as activation of free carriers leading to plasmon-phonon coupling (Fig. 2). With the knowledge of the phonon mode line shift with temperature (Fig. 3(a)), we can calibrate the LOPC and calculate the phonon-plasmon contribution (Fig. (3b)). Then we can define the free carrier concentration evolution.

Based on Eq. (1), we have determined the temperature dependence of free carrier concentration (Table 1).

$$n = 1.23 * 10^{17} * (\omega_{LOPC} - 964.1), \qquad (1)$$

where ω_{LOPC} is the LOPC mode position, 964.1 cm^{-1} is the theoretical position of the LO phonon mode [5].

Table 1. Temperature profile of free charge concentration obtained from Eq. (1).

Temperature (K)	Free carrier concentration (cm^{-3})
4.6	9.705×10^{17}
15	9.717×10^{17}
30	1.047×10^{18}
60	1.058×10^{18}
90	1.160×10^{18}
150	1.264×10^{18}
200	1.580×10^{18}
250	1.842×10^{18}
300	2.084×10^{18}

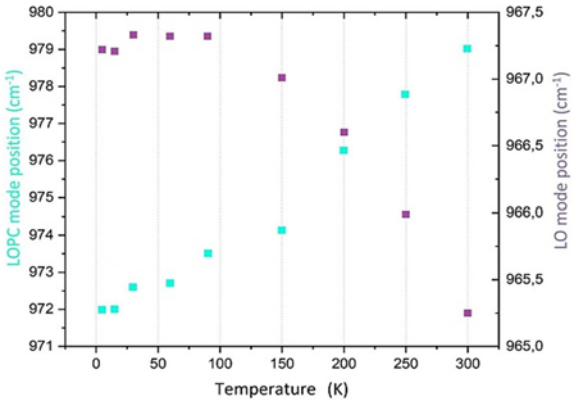

Fig. 2. LO and LOPC modes position as a function of temperature.

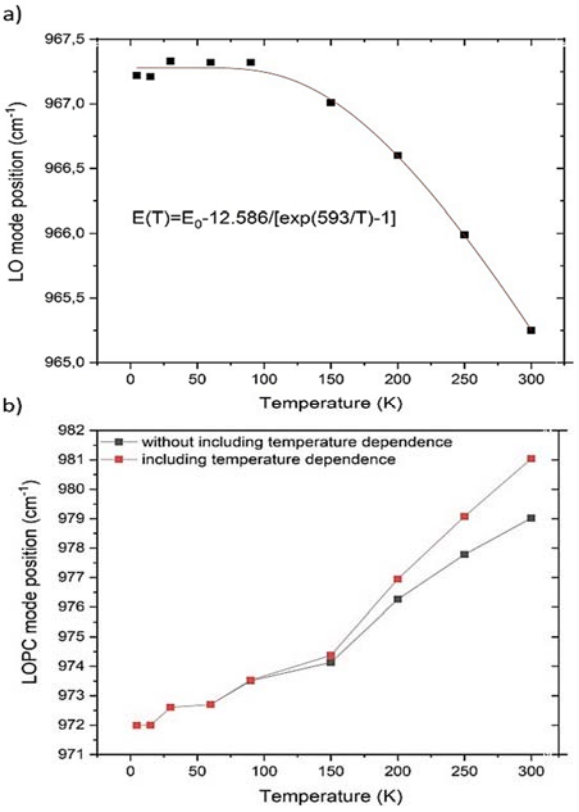

Fig. 3. (a) LO mode position as a function of temperature with a fitted curve based on a formula from [10], fitting parameters are shown on the picture. (b) LOPC mode position with and without thermal expansion (obtained in panel (a)).

2.2. Electron Transitions in Nitrogen Donors by Raman Spectroscopy

The 4H-SiC polytype contains 4 Si-C lattices (hexagonal and cubic) in its primitive unit cell. In a structure like this, donors can occupy one of the two inequivalent C-lattice sites (hexagonal or cubic). Each site has different binding energy and different structure of excited states. With knowledge of these parameters it's possible to design layers with controlled properties (such as junction capacitance of

the mentioned diodes). A number of articles refer to electron transition effects observed with Raman spectroscopy [6, 7]. Unfortunately this problem has not been carefully studied for 4H polytype and our results do not correspond exactly to the data from IR spectra [8]. At low temperatures were observed invisible in higher temperatures modes (lines signed as A, B and C in Fig. 4), which were assigned to electron transitions in donors.

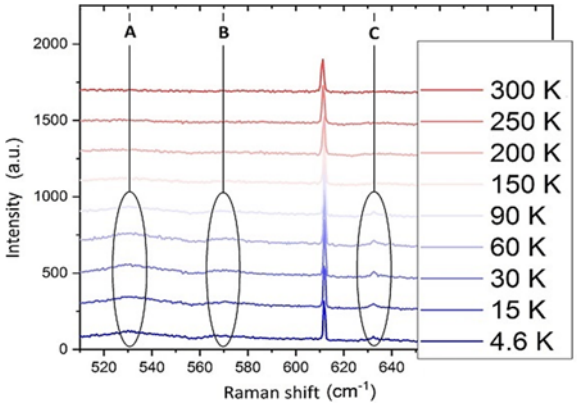

Fig. 4. Raman spectra of 4H-SiC taken separately as a function of temperature between 4.6 and 300 K. Lines A, B and C are marked. This modes are visible at low temperatures, especially in the range between 4.6 K (beginning) and 90-150 K (vanishing).

In the case of nitrogen located in the hexagonal site, there is valley orbit splitting of ground state to 1s(A_1) and 1s(E), caused by the band structure anisotropy. In article [6] the presented energy level scheme of nitrogen donors mentions valley orbit splitting on hexagonal ground state around 60 cm^{-1} and ionization energy at 438 cm^{-1}. In this work the featured A, B and C lines disappeared between 90 and 150 K (corresponding to thermal energy between 7.8 and 12.9 meV), which proves the thermal depopulation of 1s(A_1) state (splitting energy). Additionally there was no thermalization between splitted ground states (thermal disappearance affect all modes at the same time), which indicates that this Raman spectrum depicts transition from one splitted state only. Based on literature and simple calculations we obtained (Fig. 5), a splitting energy in this materials of 86.8 cm^{-1} (10.8 meV), which corresponds to temperature of 125 K. It is possible to attribute A, B, C lines to a specific transition by scaling the levels scheme from Fig. 5(a) to the obtained splitting energy. Following this, mode A (531 cm^{-1}) was assigned to transition 1s(A_1)→2$p_{\pm}$, mode B (576 cm^{-1}) to transition 1s(A_1)→3$p_{\pm}$ and mode C (632.5 cm^{-1}) to transition from 1s(A_1) to one indeterminate discrete state. Both A and B modes are related to transition between the same symmetry of initial and final states. Such modes have similar shapes. Mod C differs from the previous ones as it has different final state, which is visible in the spectrum. The ionization energy is not much above the C transition energy (around 80 meV).

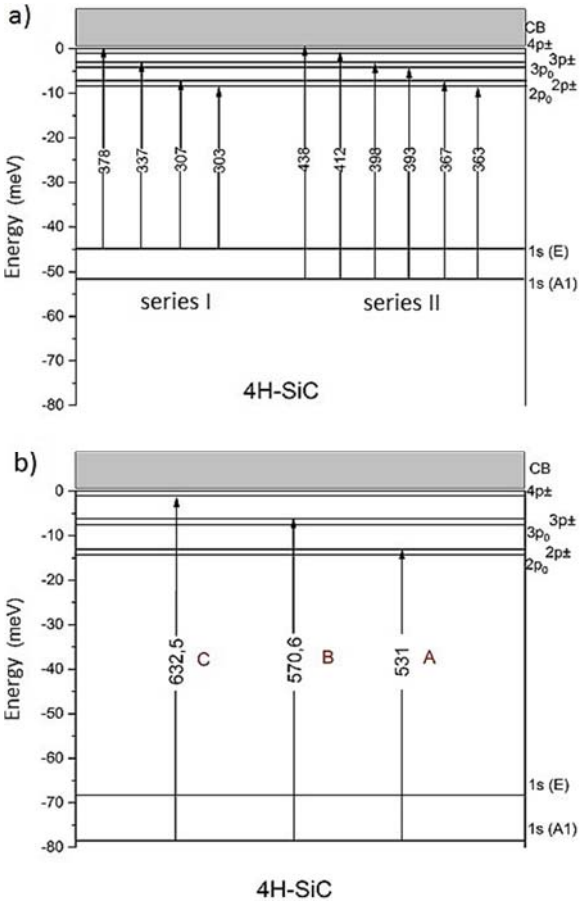

Fig. 5. (a) Energy levels scheme of nitrogen donors according to [6]; (b) Scaled (to splitting energy) energy scheme for measured material. Lines of Raman spectrum are marked.

Another effect observed at low temperatures was the appearance of an asymmetric peak related to Fano interference. The peak's asymmetry and deformation are caused by the overlapping and interference between a broad electronic state and a discrete phonon state. The mode presented in Fig. 6 is a result of interference between a folded mode FTA(E_2) and the electronic continuum [5]. A well-known Fano profile can be fitted with:

$$I = \frac{(q+\varepsilon)^2}{1+\varepsilon^2}, \tag{2}$$

where q is an asymmetric parameter, $\varepsilon=(\omega-\Omega-\delta\Omega)/\Gamma$, ω is the Raman shift, Ω is the phonon frequency, $\delta\Omega$ is the mode shift, Γ is a widening parameter related to the interference. Obtained parameters are depicted on Fig. 6.

2.3. Layer Thickness by Raman Spectroscopy

Determination of a layer thickness by SEM requires that the sample is broken to get its cross-section and image its surface. Unfortunately, this method is destructive.

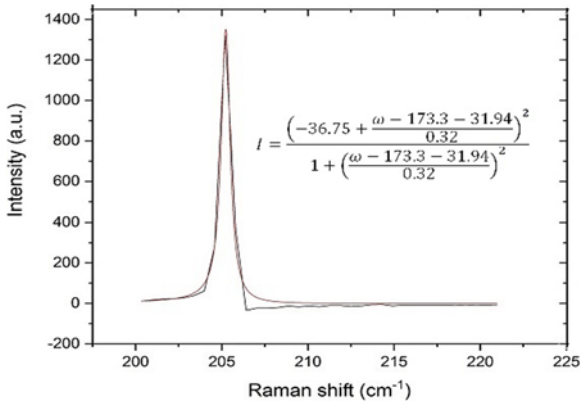

Fig. 6. Fano interference at low temperatures. This figure contains the Fano formula for the red fitting.

An excellent alternative is to study a depth profile obtained with Raman spectroscopy and a series of measurements within the bulk of the sample. This method does not destroy the sample and not only reveals the layer thickness, but also the free carriers concentration, tension and much more. Light-based methods allow for more than just surface investigations. If the material is transparent for the incident wavelength, it is possible to focus the beam under the surface. In a depth profiling the sample's refractive index should be considered. It is changing the real depth of focusing and depth resolution, referred to later as DR [9]. The value of DR is given by Eq. (3). It depends on the depth of measurement (Δ), the numerical aperture (NA) and the refractive index (n).

$$DR = \Delta * \left(\sqrt{\frac{NA^2(n^2-1)}{(1-NA^2)} + n^2} - n \right) \qquad (3)$$

In order to determine the layer thickness, significant difference in free carrier concentration between substrate and the epi-layer should be considered. In this case, the LOPC mode position in a depth profile must be measured. The boundary between layers will be characterized by a smooth transition, related to nitrogen diffusion during the epitaxial growth, resolution capability of the laser spot and the mentioned depth resolution value (DR). Fig. 7 shows an exemplary depth profile for the epi-layer and substrate. There have been two points marked, which are dividing the plot into three regions. The external areas refer to regions where the scattered light was collected only from one layer (epi-layer or substrate). In the middle region, scattered light was collected from both layers because of the DR. Going into the bulk of the sample, a laser beam is focused on a depth of Δ×n (where Δ is a given depth of measurement and n is the refractive index). In total it gives the effective working range. When the front of the working range is passing through the boundary between the layers (Point 1 in the Fig. 7), the collected light originates from both layers. After crossing the distance equal to DR, the effective working range moves to the substrate, and the light is collected only from the substrate.

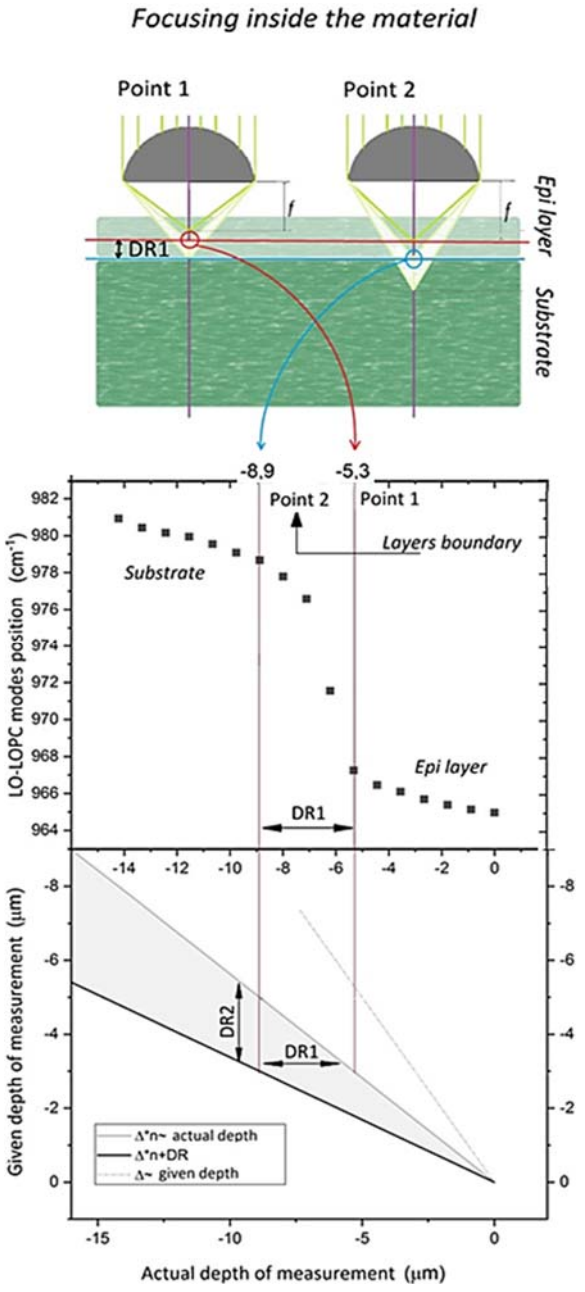

Fig. 7. Measuring the layer thickness with the help of a depth profile obtained with Raman spectroscopy. The actual depth of measurement depends on the refractive index and the given depth of measurement.

The actual depth of focus and the DR value depend mainly on the refractive index, which in practice turns different from literature values [9]. The real value of the refractive index can be determined based on the knowledge of Point 1 and Point 2, and by solving the below featured equation:

$$\Delta_1 \times n + DR(\Delta_1, n) = \Delta_2 \times n \Rightarrow n = \frac{DR(\Delta_1, n)}{\Delta_2 - \Delta_1}, \qquad (4)$$

where $\Delta_1(\Delta_2)$ is the given depth of measurement in Point 1(2), and n is the refractive index.

2.4. SIMS and Raman Depth Profiles

Tracing the position of LOPC mode at room temperature, we have measured depth profiles and changed the position of the focal plane inside the sample. It provided information on the free electrons concentration gradient within the layers interface (Fig. 8 (b)). Knowing that the epitaxial and substrate free carriers concentrations are different, we have estimated the epi-layer thickness. The obtained results were compared with SIMS depth profiles of nitrogen atoms concentration and SEM cross sections showed in the background of Fig. 8 (a).

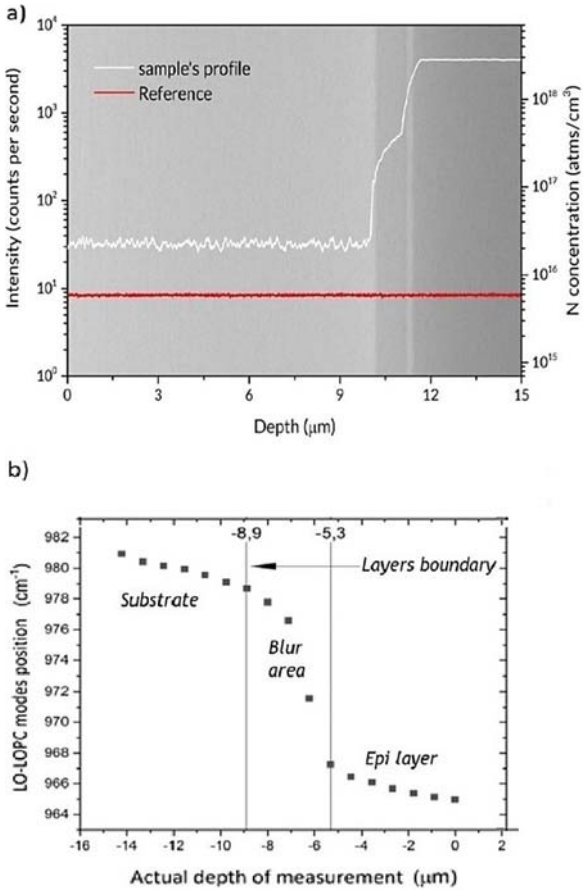

Fig. 8. (a) SIMS profile of nitrogen atoms concentration within the sample; (b) Raman depth profile of the LOPC mode position (free electron concentration and layer thickness).

It's worth mentioning that SEM measurements require that the sample is broken to measure the cross section. It involves the sample's destruction. The same problem is in SIMS, where the chemical elements are dislocated by ions.

Fig. 8 (b) depicts a single depth profile. It only provide approximate, tentative information about the sample. In order to obtain more information, it is necessary to collect data from a larger area and make a line depth profile comparable to a cross section. It provides information on the homogeneity of the layer thickness over a larger distance. This method seems to be perfect for materials investigation before sale. It helps to define under-surface profiles. Fig. 9 shows an exemplary depth slice, taken at a distance of about 30 μm with 1-μm steps. At each point there was a depth profile taken. The layer boundary is on the sharp line, what indicates uniformity in thickness. The obtained image should be scaled according to Eq. (4), using the numerical methods.

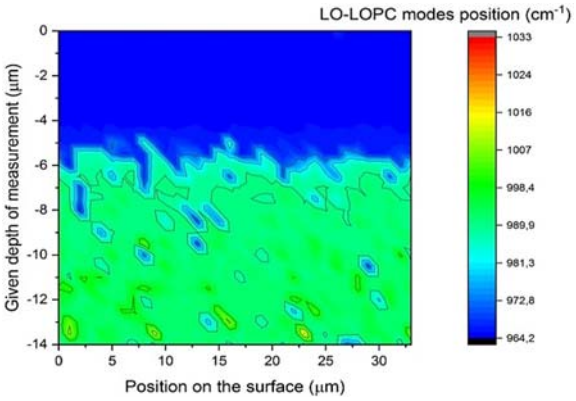

Fig. 9. A line depth profile of the sample measured with Raman spectroscopy. The X and Y axes describe the depth of measurement and the linear position. The third dimension is the LO-LOPC modes position. There is a significant change of modes position on one sharp line.

3. Conclusions

In this work were measured few parameters of 4H-SiC, a material for power devices application. At low temperatures two effects were observed. The first one was related to the thermal expansion of the crystal and the second one to the thermal activation of nitrogen donors. Another thing observed at low temperatures was the electron transition between nitrogen donors. Based on this, we assigned specific transitions to the observed lines and find out the valley-orbit splitting and ionization energies. Additionally, there was Fano interference witnessed resulting from the overlapping of a broad electronic state and a discrete phonon. By following the longitudinal optical phonon mode and its coupling with plasmon, it is possible to determine the free carrier concentration, and based on this parameter the epi-layer thickness. Raman spectroscopy is a non-destructive, quick and useful tool to determine the free carrier concentration as a function of temperature and the epi-layer thickness.

Acknowledgements

The research leading to these results has received funding from the National Centre for Research and Development under Grant Agreement

No. TECHMATSTRATEG1/346922/4/NCBR/2017 for project "Technologies of semiconductor materials for high power and high frequency electronics" and under Grant Agreement No. LIDER 0168/L-8/2016 for project "Graphene on silicon carbide devices for magnetic field detection in extreme temperature conditions".

References

[1]. A. Dobrowolski, J. Jagiełło, W. Kaszub, T. Ciuk, K. Kościewicz, P. Michałowski, P. Ciepielewski, A. Wysmołek, A. Chamryga, P. Kamiński, Temperature investigation of phonon-plasmon modes in 4H-SiC Shottky diodes for power electronic devices, in *Proceedings of the 2nd International Conference on Microelectronic Devices and Technologies (MicDAT'2019),* Amsterdam, The Netherlands, 22-24 May 2019, pp. 63-65.

[2]. K. Kościewicz, W. Strupiński, D. Teklińska, K. Mazur, A. Olszyna, Epitaxial growth on 4H-SiC on-axis, 0.5°, 1.25°, 2°, 4°, 8° off-axis substrates – defects analysis and reduction, *Materials Science Forum,* Vol. 679-680, 2011, pp. 95-98.

[3]. K. Kościewicz, W. Strupiński, W. Wierzchowski, K. Wieteska, A. Olszyna, Polytypism study in SiC epilayers using electron backscatter diffraction, *Materials Science Forum,* Vol. 645-648, 2010, pp. 251-254.

[4]. K. Kościewicz, R. Bożek, W. Strupiński, A. Olszyna, Microscopic investigation of SiC epitaxial layers on on-axis 4H-SiC substrates using Kelvin Probe Force Microscopy, *Acta Physica Polonica A*, Vol. 116, 2009, pp. 69-70.

[5]. S. Nakashima, H. Harima, Raman investigation of SiC polytypes, *Physica Status Solidi A*, Vol. 162, Issue 1, 1997, pp. 39-64.

[6]. W. Götz, A. Schöner, G. Pensl, W. J. Choyke, R. Stein, S. Leibenzeder, Nitrogen donors in 4H-silicon carbide, *Journal of Applied Physics,* Vol. 73, 1992, pp. 3332-3338.

[7]. J. C. Burton, F. H. Long, I. T. Ferguson, Resonance enhancement of electronic Raman scattering from nitrogen defect levels in silicon carbide, *Journal of Applied Physics,* Vol. 86, Issue 4, 1999, pp. 2073-2077.

[8]. W. Suttrop, G. Pensl, W. J. Choyke, R. Stein, S. Leibenzeder, Hall effect and infrared absorption measurements on nitrogen donors in 6H-silicon carbide, *Journal of Applied Physics,* Vol. 72, Issue 8, 1992, pp. 3708-3713.

[9]. Neil Everall, Depth profiling with Confocal Raman Microscopy, part II, *Spectroscopy,* Vol. 19, Issue 10, 2004, pp. 16-24.

[10]. K. P. Korona, A. Wysmolek, K. Pakula, R. Stepniewski, J. M. Baranowski, Exciton region reflectance of homoepitaial GaN layers, *Appl. Phys. Lett.,* Vol. 69, Issue 6, 1996, pp. 788-790.
